European Journal of Wood and Wood Products (2024) 82:69–79
https://doi.org/10.1007/s00107-023-01994-9

ORIGINAL ARTICLE

Aging effects on the viscoelastic behaviour of products by fused deposition modelling (FDM) made from recycled and wood-filled polymer resins

Antonella Patti[1] · Stefano Acierno[2] · Gianluca Cicala[1] · Domenico Acierno[3]

Received: 16 April 2023 / Accepted: 11 September 2023 / Published online: 25 September 2023
© The Author(s) 2023

Abstract
In this work, we analyse the thermal aging effects on the thermo-mechanical properties of bio-based specimens realized using fused deposition modelling technology. For the investigations, three commercial filaments made of polylactide acid (PLA) were used. The first filament was a pure virgin PLA (B-PLA); the second one was made from recycled waste production, PLA (R-PLA), and the third one was wood-filled PLA (W-PLA). Such materials were extruded under pre-optimized conditions and thermally aged in an oven at 70 °C. The as-prepared specimens were subjected to dynamic mechanical analysis (DMA) and infrared spectroscopy (IR). The experimental results are presented in terms of storage modulus (E'), loss modulus (E''), tan delta, and absorption spectra at different aging periods (0, 50, 70, 130, 175 days). For B-PLA and R-PLA, the thermal aging results in a decrease in both storage and loss moduli and in an increase in the glass transition temperature (T_g). On the contrary, for the W-PLA the storage modulus increases with the aging time, while the T_g remains constant. The IR spectra support the hypothesis of a degradation mechanism involving hydrolysis and/or hydrogen atom transfer. Based on these observations, we conclude that heat treatments always lead, through polymer degradation and structural changes, to more stable structures. The presence of wood particles slows down the aging process and makes the final products more durable.

1 Introduction

The concept of biodegradability in polymers is gaining popularity due to the incompatibility of polymeric waste with the environment where it is disposed of after use (Luckachan and Pillai 2011). Different strategies were explored to develop bio-based degradable plastics, i.e. biopolymers, that do not pollute the environment and may be used in place of oil-based traditional polymers (Nampoothiri et al. 2010).

Biopolymers can be made from polysaccharides, proteins, lipids, and bacterial activities (i.e., polyhydroxyalkanoates), conventional synthesis of bio-derived monomers (i.e., polylactides) or synthetic monomers (i.e., polycaprolactone). A wide range of biodegradable polymers has been developed for a variety of applications. Polyhydroxyalkanoates (PHA), produced in the form of granules by various microorganisms, are attractive materials for biomedical applications due to their unique properties such as biodegradability, biocompatibility, and non-toxicity (Sharma et al. 2021). Polycaprolactone (PCL) is approved for use in biomedical devices due to its low degradation rate, high ductility and plasticity (Sachan et al. 2022). Polylactic acid (PLA) is an aliphatic polyester, considered a "green" ecological material (Nampoothiri et al. 2010).

PLA is currently the most promising and commonly used biopolymer in various industries like packaging, textiles, construction, and automotive (Nofar et al. 2019). Being thermoplastic in nature, PLA can easily be processed with traditional technologies in extrusion, compression moulding,

✉ Antonella Patti
antonella.patti@unict.it

Stefano Acierno
stefano.acierno@unisannio.it

Gianluca Cicala
gianluca.cicala@unict.it

Domenico Acierno
acierno@crdctecnologie.it

[1] Department of Civil Engineering and Architecture (DICAr), University of Catania, Viale Andrea Doria 6, 95125 Catania, Italy

[2] Department of Engineering, University of Sannio, Piazza Roma 21, 82100 Benevento, Italy

[3] Regional Center of Competence New Technologies for Productive Activities Scarl, Via Nuova Agnano 11, 80125 Naples, Italy

injection moulding, and thermoforming (Cisneros-López et al. 2020). PLA is also used in the, more recent, additive manufacturing (AM) technologies; in particular, in the fused deposition modelling (FDM), due to its biodegradability, good mechanical properties, and low crystallization rate (Patti et al. 2022a, b, c, 2023). The latter is a crucial aspect for promoting interlayer adhesion in 3D printed parts. The low melting point of PLA makes this polymer very attractive in order to reduce the energy consumption in 3D printing (Cisneros-López et al. 2020).

At high temperatures during thermal processing or under hydrolytic conditions PLA macromolecules can break down resulting in a decrease in molecular weight (Signori et al. 2009). The effect of extrusion parameters, such as temperature and screw speed, on the structure and properties of various PLA grades was investigated in Mysiukiewicz et al. (2020). The results showed that during extrusion at high temperature (up to 260 °C) and screw speed (up to 250 rpm), the polymer underwent thermo-mechanical and thermo-oxidative degradation (Mysiukiewicz et al. 2020). According to a large amount of published data, PLA thermal degradation was caused by random main-chain scission reactions, depolymerization, oxidative degradation, and transesterification processes (Signori et al. 2009). As a result, the PLA properties were degraded due to permanent physical and chemical changes of the molecular structure or continuous evolutions to achieve a stable configuration of thermodynamic equilibrium (Budin et al. 2019). Such structural changes consisted of permanent chemical changes and breaking of primary atomic bonds, leading to irreversible material changes (Hutchinson 1995).

Often in common polymer processing the materials are rapidly cooled from high temperatures, thus giving rise to non-equilibrium state. Physical aging, or structural relaxation, refers to conformational changes that the polymer chains undergo after processing towards a thermodynamically stable state (Chandra et al. 2018). Physical aging refers only to reversible changes in chemical or physical properties, and results in a decrease in free volume, an increase in glass transition temperature, an increase in stiffness and a decrease in deformability (Cui et al. 2020).

In addition to physical aging other factors, such as the presence of water and crystallization, can also affect the final properties of PLA-based products. Hydrolysis, occurring in the presence of water, reduces the molecular weight and increases the brittleness (Cui et al. 2020). However, hydrolysis is very slow at room temperature and in the absence of catalysts (Cui et al. 2020). It was demonstrated that physical aging of the PLA structure occurred under differed humidity conditions (immersion in water, 50 or 100% relative humidity) at 50 °C (Rocca-Smith et al. 2017). At temperatures below the glass transition, slow molecular rearrangements in amorphous polymers tended to lower free energy and free volume. This resulted in a gradual densification of the polymer structure, which became more glassy and less rubbery. Temperatures close to T_g accelerated the rearrangement of these molecules (Rocca-Smith et al. 2017).

The recyclability of biopolymers is critical for their long-term and cost-effective use. Recycling has proven to be a valuable tool in solving environmental and waste management problems (Shojaeiarani et al. 2019). Mechanical and thermal properties of PLA after five cycles of extrusion and moulding were measured (Shojaeiarani et al. 2019). Compared to virgin PLA, the recycled polymer in the glassy state exhibited a 7.25% smaller decrease in storage modulus and a higher dissipation factor. This indicated the viscous rather than elastic nature of the material (Shojaeiarani et al. 2019). Budin et al. (2019) investigated the mechanical properties of recycled PLA from the injection moulding process. The results showed that the recycled PLA had 11% lower tensile strength, 4% lower hardness and 50% lower impact strength than virgin PLA. The reduced mechanical performance was attributed to thermal degradation of the PLA molecular chains during the injection moulding process.

The presence of various amounts of flax fibers (up to 30%) in the polymer matrix led to reversible (i.e., plasticization) and irreversible (i.e., damage) changes, affecting the mechanical properties of PLA-based biocomposites during aging. Chain mobility increased with increasing the water content and temperature. The ability of molecules to migrate further increased the water absorption within the polymer. The lignocellulosic materials have a high affinity for water, which enhances the moisture storage capacity and diffusion rate of water within the biocomposites. The swelling that takes place during water absorption and desorption damages the flax fibers, causing hoop stress, plastic strain and microcracks in the matrix. However, fibers did not always provide a high degree of irreversibility. Indeed, with long-term aging, fibers have shown to delay PLA failure and extend the life of the material (Regazzi et al. 2016). Then, wood particles can slow down the diffusion of degradation products from the polymer bulk to the gas phase and thus protect the polymer from thermal decomposition (Patti et al. 2021).

Polymer degradation is often an uncontrollable process that cannot be stopped even if the material is kept isolated from the aggressive environment in a stress-free state. By amplifying one or more environmental parameters that characterize actual exposure, aging becomes a useful method to predict durability and long-term properties of polymeric materials (Frigione and Rodríguez-Prieto 2021).

In this study, in order to validate the durability of bio-based materials for 3D-printing applications, we investigate the effects of long-term exposure to high temperatures on the thermo-mechanical properties of PLA-based 3D-printed specimens. To this end, a virgin PLA polymer, a recycled PLA, and a wood/PLA composite were used to

prepare specimens by additive manufacturing. The thermal aging was conducted in an oven at 70 °C for up to 4200 h (175 days); such conditions could correspond to about 10–15 years of real service time (Hukins et al. 2008; Yarahmadi et al. 2016; Bergaliyeva et al. 2022). Infrared spectroscopy was used to confirm chemical changes in the materials and to validate the potential adverse effects of thermal degradation due to aging.

2 Materials and methods

2.1 Materials

For the experimental campaign we have used three different filaments with a nominal diameter of 1.75 mm. In particular, two types of unfilled PLA, one from virgin granules (B-PLA) and one recycled from filaments waste production (R-PLA); the third one was a composite made from PLA and fir wood pulp (W-PLA). All the filaments were supplied by Eumakers (Barletta, Italy). According to manufacturer information, the basic PLA polymer (cod. IngeoTM Biopolymer 4032D) was supplied by Natureworks (Minnesota, USA). Preliminary thermal analysis confirmed that the composite system contained at least 20% wood by weight (Patti et al. 2022c).

2.2 Sample preparation

These filaments were extruded in a 3D printer (code M200, by Zortax, Olsztyn, Poland) using pre-optimized conditions (Patti et al. 2022b). Z-Suite was printer management software. All filaments were dried in an oven at 70 °C for 5 h prior to the printing to remove any trace of moisture. Rectangular 3D printed specimens, 2 mm thick, 5 mm wide and 25 mm long, were manufactured for thermo-mechanical testing. Table 1 summarizes the processing conditions expressed in terms of temperature, speed, and geometrical parameters used for each material. In general, smaller layer thickness allows to obtain specimens with higher mechanical strength and higher quality (i.e., less visible layer distinction) (Patti et al. 2022a). The B-PLA and R-PLA filaments were extruded at the smallest possible layer thickness (0.09 mm). In this same condition, W-PLA printing encountered frequent nozzle clogging. The layer thickness was increased to 0.19 mm in order to provide a continuous flow of the molten composite through the nozzle, while the retraction speed and distance were reduced compared to the setting used for B-PLA and R-PLA printing.

Table 1 Optimized processing conditions for 3D printing

Technological variables	B-PLA and R-PLA	W-PLA
Layer thickness	0.09 mm	0.19 mm
Nozzle diameter	0.4 mm	0.4 mm
Infill percentage	100%	100%
Platform temperature	70	70
Nozzle temperature	210 °C	210 °C
Printing speed	Default	Default
Retraction speed	27 mm/s	20 mm/s
Retraction distance	2.7 mm	1 mm

Accelerated aging was performed in an oven at 70 °C for up to 4200 h (corresponding to 175 days/6 months). During aging, the samples were supported by wire mesh. According to the so-called "ten degree rule" a 10 K temperature increase doubles the rate of degradation and halves the material's duration (Yarahmadi et al. 2016). A common method (Hukins et al. 2008) to evaluate the effect of the aging temperature on time considers that the aging rate increased by a factor, f, equal to:

$$f = 2^{\frac{\Delta T}{10}} \tag{1}$$

where ΔT is the difference between the aging temperature and the reference temperature (i.e., the service temperature). For a material that will endure its entire life at 20 °C, maintaining the material for 1 month at 70 °C would equate to an aging of $2^{(70-20)/10} = 2^5 = 32$ months.

3 Characterization techniques

3.1 Dynamic mechanical analysis (DMA)

The machine used for dynamic mechanical analysis was the Tritec 2000 DMA manufactured by Triton Technology Ltd. (Leicestershire, UK). The instrument was operated with a single cantilever holder and 10 mm sample length, a heating rate of 2 °C/min, a maximum displacement of 0.05 mm, and a frequency of 1 for all the samples. The temperature was controlled by a thermocouple placed near the sample. DMA measurements were performed from room temperature to 80 °C in air. Initially, the sample was blocked between the two clamps. During scanning, one clamp stays stationary, whereas the other oscillates sinusoidally. The viscoelasticity of a material is determined by applying an input and measuring the response of the material. Under linear conditions the stress (σ) and strain (ε) are both sinusoidal function of time (t) with the same frequency (ω), according to the following relations:

$$\sigma(t) = \sigma_0 \sin(\omega t + \delta) \tag{2}$$

$$\varepsilon(t) = \varepsilon_0 \sin(\omega t) \tag{3}$$

where σ_0 is the stress amplitude, ε_0 is the strain amplitude and δ is the phase shift between force and displacement (δ = 0° correspond to a perfect elastic, Hookenian, material; δ = 90° to a pure viscous, Newtonian, material).

Stress and strain are linked by the complex modulus (E*):

$$\sigma(t) = E^*(\omega)\varepsilon(t) \tag{4}$$

The complex modulus (E*) is determined from measured data and geometry of the sample (Stark 2013). E* can be split in the two components (storage modulus-E′, and loss modulus-E″):

$$E\prime = \frac{\sigma_0}{\varepsilon_0} cos\delta \tag{5}$$

$$E'' = \frac{\sigma_0}{\varepsilon_0} sen\delta \tag{6}$$

The storage modulus represents the elastic response of the material and is related to the energy stored per cycle. The loss modulus represents the viscous response of the material and refers to the loss, or dissipated, energy per cycle. The glass transition temperature is commonly detected as the temperature corresponding to the peak of the dissipation factor curve (tan delta). Tan δ is the ratio between the loss and the storage modulus $\left(tan\delta = \frac{E\prime\prime(\omega)}{E\prime(\omega)}\right)$ (Goertzen and Kessler 2007).

3.2 Attenuated infrared spectroscopy (ATR)

A spectrometer (model Spectrum 65 FT IR) produced by Perkin Elmer (Waltham, MA, USA), was utilized to perform infrared spectroscopic analysis on aged specimens in attenuated total reflectance (ATR) mode. During the investigation, the infrared light passed through a diamond crystal on which the sample was placed. The background spectra are collected using free crystal. A wavenumber range of 650–4000 cm^{-1}, a resolution of 4 cm^{-1}, and a scan number of 16 were used for the test. Three measurements were performed on each specimen, and a representative curve was considered for direct comparison between the ATR spectra. Each curve was normalized considering an internal standard for PLA polymer at 1455 cm^{-1}. This signal is a characteristic peak of the asymmetric bending vibration for the methyl group (CH_3).

4 Experimental results

4.1 Visual changes in samples after heat treatment

As changes in the physical appearance of aged materials can be investigated visually, photographs of the specimens (prior and after heat treatment) are presented in Fig. 1.

From inspection of Fig. 1 we can observe that for B-PLA and R-PLA an exposure to the most severe aging condition (70 °C for 175 days) produced insignificant variations in the color intensity and gloss of the samples without noticeable yellowing. However, for these materials, the heat treatment caused visible deterioration such as sagging and permanent deformation. On the contrary (see Fig. 1c), the wood-based resin W-PLA, subjected to the same thermal treatment, shows no signs of deterioration, with stable color, and undeformed specimens.

Mass variations, measured during the aging process, can be used to monitor decomposition processes as eventual mass loss is due to releases of volatile species into the environment (Andersson et al. 2012).

The mass and thickness of samples are reported as a function of the aging days in Table 2. All the systems show irrelevant (as within the experimental error) variations in both mass and thickness up to 175 days of heat treatment. It should be noticed that the wood-based systems are lighter than that of pure PLA's. This can be attributed to various reasons including: (i) the wood flour has a lower density (190–200 kg/m^3 (Pokhrel et al. 2021)) compared to PLA polymer (1200–1400 kg/m^3); (ii) the removal of the pure PLA samples from the support base is more difficult compared to wood composites and some residues of material were left on the underside; (iii) the layer thickness required to print wood-based filaments is greater compared to the layer thickness used to print unfilled polymers (0.19 vs 0.09 mm).

4.2 Viscoelastic properties of aged 3D specimens

Figure 2 shows DMA results for virgin, neat, resin (B-PLA), in terms of storage modulus (E′), loss modulus (E″) and tan delta curve as a function of the temperature.

Fig. 1 Specimens before and after aging for: B-PLA **a**, R-PLA **b**, W-PLA **c**

Table 2 Mass and thickness for aged specimens

	B-PLA		R-PLA		W-PLA	
	Mass (mg)	Thickness (mm)	Mass (mg)	Thickness (mm)	Mass (mg)	Thickness (mm)
0 days	375 ± 7	2.83 ± 0.04	371 ± 31	2.88 ± 0.06	293 ± 2	2.22 ± 0.01
50 days	374 ± 6	3.08 ± 0.17	369 ± 25	3.00 ± 0.13	290 ± 2	2.28 ± 0.07
70 days	376 ± 8	2.85 ± 0.04	382 ± 23	2.95 ± 0.02	286 ± 12	2.19 ± 0.16
130 days	383 ± 14	3.07 ± 0.25	388 ± 10	2.81 ± 0.07	293 ± 1	2.24 ± 0.15
175 days	377 ± 10	3.01 ± 0.12	379 ± 8	3.17 ± 0.17	295 ± 1	2.28 ± 0.06

At low temperature (i.e., lower than the glass transition) the polymer is in a glassy state and its storage modulus (see Fig. 2a) is significantly affected by the heat aging and shows a 30% reduction for a 175-day treatment. This behaviour is consistent with the literature where it is often observed a tensile modulus decrease with aging time and temperature. Niaounakis et al. (2011), for instance, found a significant decrease in the tensile properties of PLA samples after 100 days at 50 °C: the Young's modulus decreased by up to 51.5% and the tensile strength decreased by 65%. Water worked primarily as a degrading (hydrolysis) agent, and the shorter chains formed from PLA breakdown were rearranged in crystallites with low melting point.

The loss modulus of the B-PLA samples decreases with increasing the thermal treatment (see Fig. 2b) thus suggesting a reduction of the macromolecular ability for energy dissipation. This behaviour can be attributed to higher density and packing fraction of the amorphous regions due to the heating treatment. The PLA matrix, characterized by predominantly amorphous structure, undergoes physical rearrangements during the aging process, giving rise to a more stable organization (Pluta et al. 2008).

As aging increases, the tan delta peak (see Fig. 2c), and as a consequence the glass-to-rubber transition takes, shifts to higher temperatures. The peak height shows a slight maximum for intermediate (50, 70 and 130 days) aging times and then, for the longest thermal treatment, its intensity returns to the initial value. The glass transition temperature (T_g) of the pure polymer (B-PLA) is around 66 °C for unaged samples, it shifts to higher values (~ 71 °C for the 70-day aged samples) and lowers (~ 69 °C) for the most severe (175 days) aging conditions. Such a behaviour can be explained by the presence of two counteracting phenomena (Matečić Mušanić and Sućeska 2009): (i) densification, which prevailed during the initial aging period, reduces the flexibility of the polymer chains and produces a T_g increase; and (ii) chain scission, which dominates during the later stages, increases structural homogeneity and produces a T_g decrease.

Figures 3 and 4 show the behaviours of the R- and W-PLA, which are roughly similar to those observed for B-PLA filament.

Figure 3 shows the temperature-dependence of the viscoelastic properties (storage modulus (a), loss modulus (b), and tan delta (c)) as a function of aging duration for R-PLA. The reduction in storage modulus (E′) in the glassy region of R-PLA (see Fig. 3a) is less pronounced compared to the B-PLA and is in the range of 10%. The onset of the glass transition is always delayed in aged samples compared to the unaged material. The peak height of the E″-T curve decreases with aging duration, and the corresponding width also decreases slightly (see Fig. 3b). The entire E"-T curve moves towards higher temperatures as the aging duration is increased. The tan delta peak increases with aging time and shifts to higher temperatures (see Fig. 3c).

The temperature-dependency of the storage modulus (E′), loss modulus (E″) and dissipation factor (tan delta) for wood-based composite before and after heat aging are presented in Fig. 4. In the glassy region the storage modulus shows an increase (up to 13%) due to the aging (see Fig. 4a). On the contrary, the loss modulus peak height decreases

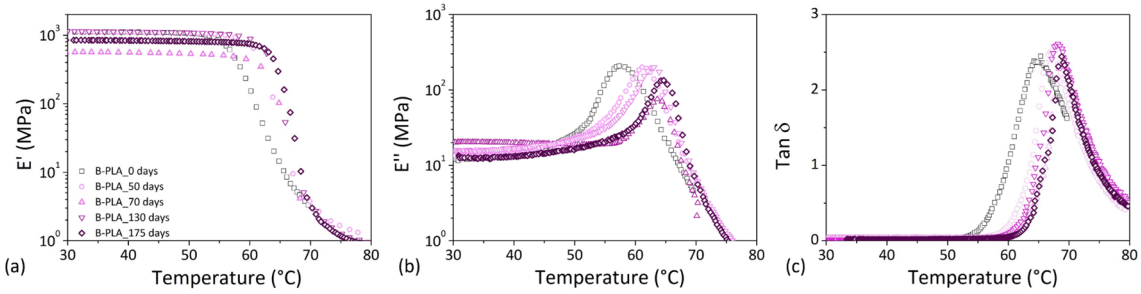

Fig. 2 DMA results for B-PLA-based printed samples: **a** storage modulus, E′; **b** loss modulus, E″; **c** dissipation factor, Tan δ. (Legend in Fig. 2b and c as in a)

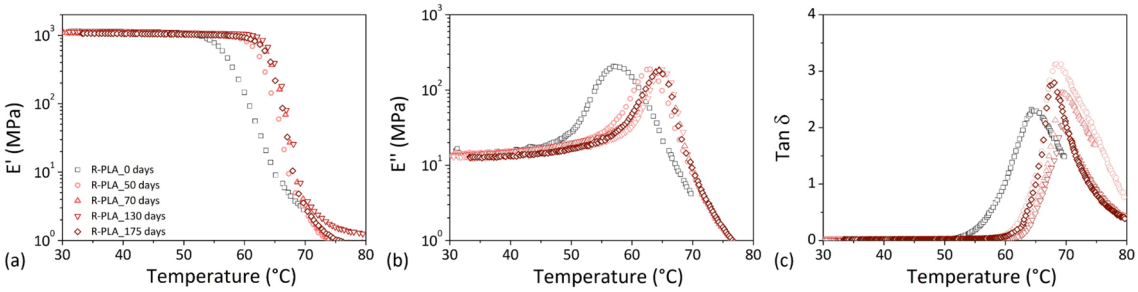

Fig. 3 DMA results for R-PLA-based 3D samples: **a** storage modulus, E′; **b** loss modulus E″; **c** dissipation factor, Tan δ. (Legend in Fig. 3b and c as in a)

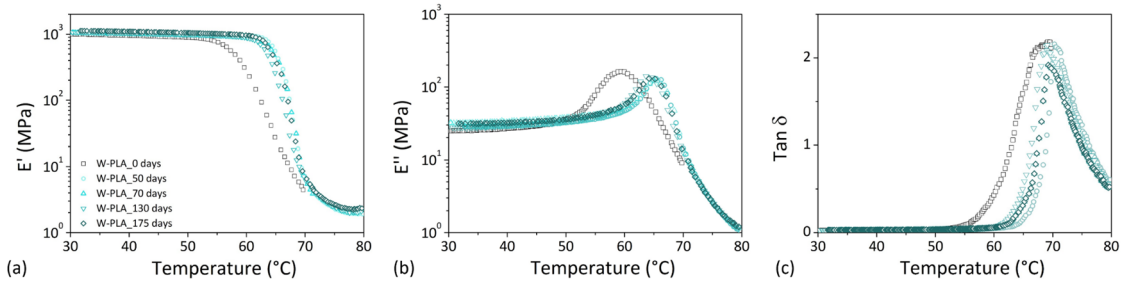

Fig. 4 DMA results for W-PLA-based 3D samples: storage modulus, E′ (**a**); loss modulus, E″ (**b**); dissipation factor, Tan δ (**c**). (Legend in Fig. 4b and c as in a)

and shifts to higher temperatures (see Fig. 4b). The glass transition temperature is only slightly affected by thermal aging with values around 70 °C (see Fig. 4c). This behaviour indicates that no significant molecular events affecting the viscoelasticity of the composites occurs during the thermal treatment (Paunonen et al. 2020). The presence of wood filler contributes to an enhancement of the mechanical properties during the aging by restricting the segmental mobility of the polymeric chains and preventing the enthalpic relaxation of PLA-based composite (Lee et al. 2020). This corresponds to a lower level of tan delta peak in the aged composites (Paunonen et al. 2020).

The increase in storage modulus during the aging can be attributed to stronger interactions at the interfaces between PLA and wood fibers or to the fibers promoting the crystallization (Paunonen et al. 2020). Hydrothermal treatment has been extensively studied to improve the wood properties. This process was found to alter the morphology, the physical and mechanical properties of treated wood. After the hydrothermal treatment, the wood samples have shown reduced presence of hydroxyl (OH^-) and carbonyl groups in the cell walls and improved dimensional stability and resistance to decay (Rowson Ali et al. 2021). In our case, long-time heat treatment above ambient temperature of PLA/wood-based composite could have determined changes in the wood surface chemistry with improved interface interactions between hydrophilic wood particles and hydrophobic biopolymer. Furthermore, particles in filled thermoplastic polymers tend to agglomerate under Brownian motion, thus forming a filler network during aging or further processing (Zhang et al. 2006). This results in increased filler/filler and filler/matrix interactions and increased overall stiffness of the aged wood biocomposites.

The average values of storage modulus (E′) at 30 °C, temperature and intensity of loss modulus peak, and temperature (T_g) and intensity of tan delta peak are summarized in Table 3.

4.3 ATR-FTIR spectroscopy on aged parts

To examine microstructural changes due to the aging, ATR-FTIR spectra were collected for each specimen and aging duration from 0 to 175 days. Aging had a qualitatively similar effect on the characteristic absorption bands of PLA polymer in all three materials. The typical bands for PLA polymer are: the stretching vibrations of hydroxyl groups (ν_{OH}) in the range of 3000–3800 cm^{-1}; C–H alkane stretching vibration ($\nu_{C\text{-}H}$) in the range of 2800–3000 cm^{-1}; carboxyl group stretching ($\nu_{C=O}$) at 1750 cm^{-1}; C–O vibration of ester group (symmetric stretching) ($\nu_{C\text{-}O}$) at 1183 cm^{-1}. The bands in the range of 1317–1425 cm^{-1} are generally assigned to various C-H vibrations (Harnnecker et al. 2012; Schramm

Table 3 E′ at 30 °C, temperature at E″ peak and intensity, T_g and peak intensity of tan delta curve for aged and unaged materials

	E′ (MPa) at 30 °C	T at E″ peak (°C)	E″ peak intensity (MPa)	T_g (°C)	Tan delta peak intensity
B-PLA					
0 days	1130 ± 108	58.0 ± 0.4	220 ± 12	65.6 ± 0.2	2.3 ± 0.1
50 days	1030 ± 151	61.8 ± 0.2	187 ± 30	67.7 ± 0.6	2.7 ± 0.1
70 days	497 ± 120	64.4 ± 0.1	74.5 ± 38	70.8 ± 3.3	3.0 ± 0.8
130 days	1190 ± 135	63.0 ± 0.3	207 ± 15	68.1 ± 0.1	2.7 ± 0.1
175 days	844 ± 228	64.5 ± 0.2	140 ± 68	69.1 ± 0.4	2.4 ± 0.1
R-PLA					
0 days	1180 ± 119	57.6 ± 0.1	209 ± 22	64.7 ± 0.4	2.2 ± 0.1
50 days	1090 ± 125	62.9 ± 0.2	189 ± 15	68.0 ± 0.5	2.7 ± 0.3
70 days	1080 ± 245	64.6 ± 0.2	181 ± 4	70.4 ± 1.9	2.3 ± 0.2
130 days	1060 ± 883	64.9 ± 0.1	175 ± 18	69.7 ± 0.4	2.1 ± 0.1
175 days	1140 ± 102	64.0 ± 0.6	197 ± 20	68.5 ± 0.6	2.9 ± 0.1
W-PLA					
0 days	1030 ± 351	60.0 ± 0.4	170 ± 70	69.5 ± 0.3	2.3 ± 0.1
50 days	1110 ± 103	66.5 ± 2.4	105 ± 62	70.5 ± 0.5	2.1 ± 0.1
70 days	1040 ± 54	65.5 ± 0.2	129 ± 26	70.8 ± 0.4	2.0 ± 0.1
130 days	1150 ± 281	63.9 ± 0.2	155 ± 37	69.2 ± 0.2	2.2 ± 0.1
175 days	1160 ± 59	64.4 ± 0.1	137 ± 4	69.3 ± 0.1	1.9 ± 0.1

2020). The anti-symmetric and symmetric stretching vibrations of C-O bonds (C–O–C, C–OH) are in the region of 890–1160 cm^{-1} (Schramm 2020).

Figure 5 shows the spectral measurements for aged and unaged samples for the B-PLA resin. Spectra allow to detect changes such as formation/disappearance and increase/decrease of various bands. After 50 days of thermal treatment (see Fig. 5a): (i) absorbance of hydroxyl band (ν_{OH}) increases significantly while the carboxyl group vibration ($\nu_{C=O}$) decreases; (ii) the C-O vibration of ester group disappears (ν_{C-O}), (iii) a new board at 1630–1650 cm^{-1} peak appears. After 70 days of thermal aging, ν_{OH} and ν_{C-H} decreases, while $\nu_{C=O}$ increases.

In general, the hydrolytic degradation of a polymer matrix takes place in two stages: (i) water diffusion into the polymer bulk and (ii) hydrolysis reaction. In contrast to thermal degradation, which requires high temperatures of 200–250 °C and a vacuum at 4–5 mmHg, hydrolysis is a relatively simple depolymerization process that does not necessitate harsh processing conditions or catalysts (Piemonte et al. 2013). Time-evolution of absorption spectra for water molecules diffusion into polycaprolactone (PCL) film were displayed in Peng et al. (2003). Two signals are representative of water absorption in the polymer: the first in the range of 3000–3800 cm^{-1} was attributed to stretching vibration of OH group (ν_{OH}) and the second in the range of 1600–1650 cm^{-1} was attributed to bending vibration of OH group. As water diffused into the PCL film, these signals gradually increased.

In our case, water (coming for moisture penetrating into the non-perfectly insulated chamber) could have diffused into specimens during aging and attacked the double carboxyl bond via the hydrolysis mechanism (Al-Itry et al. 2012). This process results in a random scission of chains.

However, the peak at 1635 cm^{-1} can be attributed to the stretching vibration of a carbon-double bond (C=C) ($\nu_{C=C}$) (Alia et al. 2018). This consideration could support the possibility of a second PLA degradation mechanism (Al-Itry et al. 2012) involving hydrogen atom transfer and the creation of terminal vinyl ester and carboxyl groups.

After 130 and 175 days of thermal treatment (see Fig. 5b), all the absorption bands of the aged specimens return to be close to those of starting material. ν_{C-H}, ν_{OH}, $\nu_{C=C}$ are slightly higher while $\nu_{C=O}$, ν_{C-O}, ν_{C-O-C} are lower compared to intensities recorded for original polymer.

Findings for B-PLA resin are confirmed for R-PLA (see Fig. 6a) and W-PLA (see Fig. 6b).

Spectroscopic analysis also provided qualitative information on the crystallinity of the samples; indeed FTIR has proved to be a promising tool to characterize crystallinity changes in materials (Abbass et al. 2021). For PLA, the two peaks at 870 cm^{-1} and 756 cm^{-1} were considered representative of the amorphous and crystalline phases, respectively (Patti et al. 2022b). Pop et al. (2019) observed a decrease in the ratio of the two band areas A_{756}/A_{861} from 3.095 for the PLA-based filament to 1.763 for the printed material. This was attributed to decrease in crystallinity during the PLA printing. Briassoulis et al. (2022) studied the mechanical

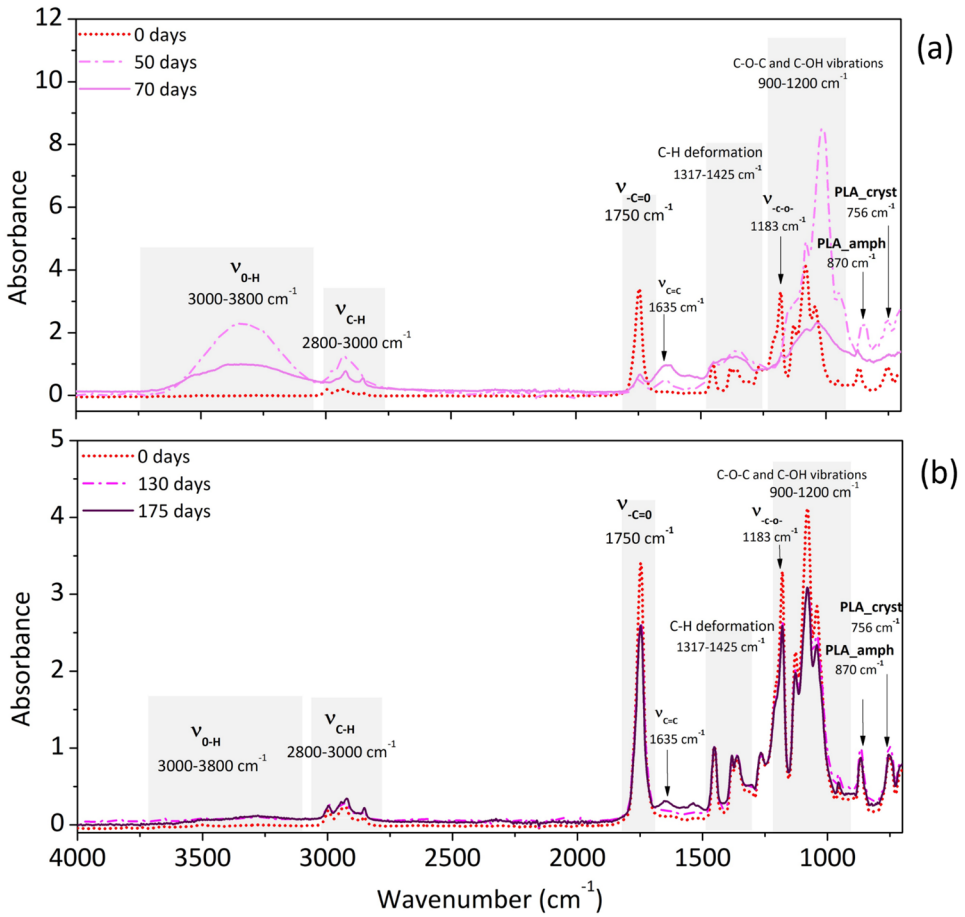

Fig. 5 ATR spectra for B-PLA at: **a** 0, 50 and 70 aging days, and **b** 0, 130 and 175 aging days

performance against physical aging of the PLA/PHB blends with olive oil and carvacrol as plasticizing and stabilising additives. The mixture displayed a higher intensity at 756 cm^{-1} peak compared to basic PLA suggesting a rise in the crystallinity of PLA's phase within the compound.

The crystallinity index (I_c) was calculated through the areas ratio of aforesaid characteristic peaks ($Area_{870}$/$Area_{756}$) (Stoleru et al. 2017) over the aging time. Data are summarized in Table 4 and suggest that changes in the crystallinity due to the aging are negligible. In all cases, the crystallinity index is close to unity thus indicating that potential densification did not affect the degree of structural order in the solid.

5 Conclusion

In this study, the thermo-mechanical performance of 3D-printed specimens made from unfilled and wood-filled PLA polymer are investigated as a function of thermal aging.

For unfilled resins subjected to thermal aging, DMA results show a decrease in E' in the glassy region, a shift to higher temperatures and a decreased intensity of E″ peak, an increase in the intensity of the tan delta peak and its shift to higher temperatures. These findings can be explained by the occurrence of two opposing mechanisms: an increment in density and packing fraction during physical rearrangement towards the equilibrium state, and a chain scission mechanism that enhances the structural homogeneity of polymer macromolecules.

For the wood-filled resin, with increasing aging days, E′ in the glassy region increases the E″ peak shifts to higher temperatures and its intensity decreases, the tan delta peak remained unchanged. The different behaviour observed for the wood composite can be attributed to a reduced chains mobility due to macromolecular compaction, particles flocculation, and networks formation of wood particles. Furthermore, the enhanced rigidity of the wood-composite can be attributed to improvements of the filler-matrix interface. ATR measurements reveal possible hydrolysis of the PLA polymer, resulting in a random chain scission, as well as a second degradation mechanism involving a hydrogen atom transfer. The analysis of crystallinity index suggests that the effect of aging on the structural order of the original material was negligible.

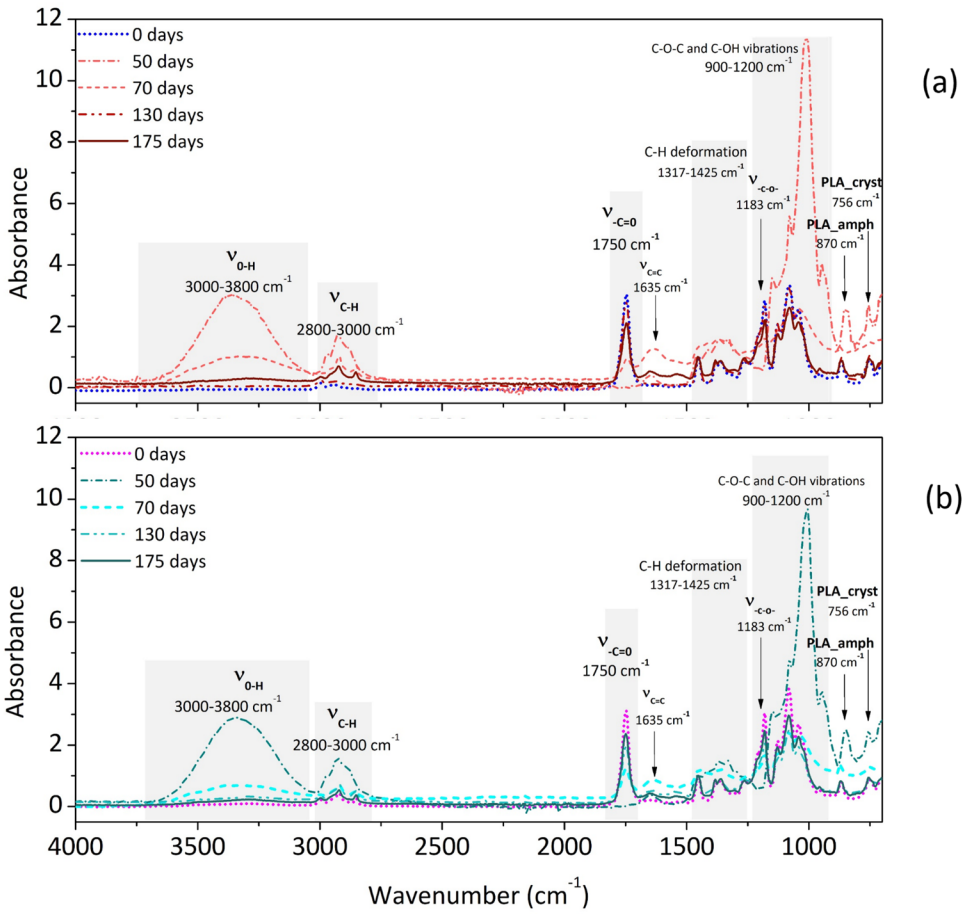

Fig. 6 ATR spectra for R-PLA **a** and W-PLA **b** at various aging days

Table 4 Absorbance intensity at 870 cm^{-1} (A_{870}) and at 756 cm^{-1} (A_{756}), and crystallinity index (I_c)

	B-PLA			R-PLA			W-PLA		
	A_{870}	A_{756}	I_c	A_{870}	A_{756}	I_c	A_{870}	A_{756}	I_c
0 days	0.848 ± 0.015	0.894 ± 0.026	0.97 ± 0.02	0.749 ± 0.017	0.831 ± 0.031	1.17 ± 0.02	0.811 ± 0.014	0.911 ± 0.009	1.22 ± 0.02
50 days	2.439 ± 0.186	2.621 ± 0.135	1.08 ± 0.00	2.529 ± 0.006	2.672 ± 0.052	1.07 ± 0.02	2.431 ± 0.058	2.538 ± 0.054	0.97 ± 0.08
70 days	1.457 ± 0.041	1.322 ± 0.154	0.99 ± 0.11	1.090 ± 0.406	0.922 ± 0.313	1.13 ± 0.07	1.019 ± 0.086	1.019 ± 0.086	1.18 ± 0.03
130 days	0.899 ± 0.071	0.918 ± 0.101	1.02 ± 0.05	0.904 ± 0.091	0.944 ± 0.090	1.12 ± 0.09	0.899 ± 0.071	0.918 ± 0.101	1.16 ± 0.04
175 days	0.899 ± 0.072	0.982 ± 0.092	1.10 ± 0.02	0.845 ± 0.084	0.903 ± 0.023	1.10 ± 0.01	0.899 ± 0.072	0.982 ± 0.092	1.17 ± 0.02

In conclusion we can affirm that the thermal aging caused polymer degradation, visible sample deformation, deterioration of mechanical properties and an increase in the glass transition temperature. The presence of wood particles in PLA mitigates such effects and improves the overall product durability.

Acknowledgements A. Patti wishes to thank the Italian Ministry of Education, Universities and Research (MIUR) in the framework of Action 1.2 "Researcher Mobility" of The Axis I of PON R&I2014-2020 under the call "AIM—Attrazione e Mobilità Internazionale". S. Acierno and G. Cicala acknowledge the support of the Italian Ministry of University, project PRIN 2017, 20179SWLKA"Multiple Advanced Materials Manufactured by Additive technologies (MAMMA)".

Author contribution Conceptualization: AP and DA, Formal analysis and investigation: AP and SA, Writing—original draft preparation: AP; Writing—review and editing: SA and GC, Resources: SA and GC, Supervision: DA.

Funding Open access funding provided by Università degli Studi di Catania within the CRUI-CARE Agreement.

Data Availability Statement The data presented in this study are available on request from the corresponding author.

Declarations

Conflict of interest The authors declare no conflict of interest.

Open Access This article is licensed under a Creative Commons Attribution 4.0 International License, which permits use, sharing, adaptation, distribution and reproduction in any medium or format, as long as you give appropriate credit to the original author(s) and the source, provide a link to the Creative Commons licence, and indicate if changes were made. The images or other third party material in this article are included in the article's Creative Commons licence, unless indicated otherwise in a credit line to the material. If material is not included in the article's Creative Commons licence and your intended use is not permitted by statutory regulation or exceeds the permitted use, you will need to obtain permission directly from the copyright holder. To view a copy of this licence, visit http://creativecommons.org/licenses/by/4.0/.

References

Abbass A, Paiva MC, Oliveira DV, Lourenço PB, Fangueiro R (2021) Insight into the effects of solvent treatment of natural fibers prior to structural composite casting: chemical. Phys Mech Eval Fibers 9(9):54. https://doi.org/10.3390/fib9090054

Ali MR, Abdullah UH, Ashaari Z, Hamid NH, Hua LS (2021) Hydrothermal modification of wood: a review. Polymers 13(16):2612. https://doi.org/10.3390/polym13162612

Alia C, Jofre-Reche JA, Suárez JC, Arenas JM, Martín-Martínez JM (2018) Characterization of the chemical structure of vinyl ester resin in a climate chamber under different conditions of degradation. Polym Degrad Stab 153:88–99. https://doi.org/10.1016/j.polymdegradstab.2018.04.014

Al-Itry R, Lamnawar K, Maazouz A (2012) Improvement of thermal stability, rheological and mechanical properties of PLA, PBAT and their blends by reactive extrusion with functionalized epoxy. Polym Degrad Stab 97(10):1898–1914. https://doi.org/10.1016/j.polymdegradstab.2012.06.028

Andersson SR, Hakkarainen M, Albertsson AC (2012) Long-term properties and migration of low molecular mass compounds from modified PLLA materials during accelerated ageing. Polym Degrad Stab 97(6):914–920. https://doi.org/10.1016/j.polymdegradstab.2012.03.028

Bergaliyeva S, Sales DL, Delgado FJ, Bolegenova S, Molina SI (2022) Effect of thermal and hydrothermal accelerated aging on 3D printed polylactic acid. Polymers. https://doi.org/10.3390/polym14235256

Briassoulis D, Athanasoulia IG, Tserotas P (2022) PHB/PLA plasticized by olive oil and carvacrol solvent-cast films with optimised ductility and physical ageing stability. Polym Degrad Stab 200:109958. https://doi.org/10.1016/j.polymdegradstab.2022.109958

Budin S, Maideen NC, Koay MH, Ibrahim D, Yusoff H (2019) A comparison study on mechanical properties of virgin and recycled polylactic acid (PLA). J Phys Conf Ser 1349:12002. https://doi.org/10.1088/1742-6596/1349/1/012002

Chandra J, Singh R, Manekar M, Minguez R, Barrenetxea L, Solaberrieta E, Lizundia E (2018) A simple approach to understand the physical aging in polymers. Eur J Phys 40(1):015502. https://doi.org/10.1088/1361-6404/aaf244

Cisneros-López EO, Pal AK, Rodriguez AU, Wu F, Misra M, Mielewski DF, Kiziltas A, Mohanty AK (2020) Recycled poly(Lactic Acid)–based 3D printed sustainable biocomposites: a comparative study with injection molding. Mater Today Sustain. https://doi.org/10.1016/j.mtsust.2019.100027

Cui L, Imre B, Tátraaljai D, Pukánszky B (2020) Physical ageing of poly(Lactic Acid): factors and consequences for practice. Polymer 186:122014. https://doi.org/10.1016/j.polymer.2019.122014

Frigione M, Rodríguez-Prieto A (2021) Can accelerated aging procedures predict the long term behavior of polymers exposed to different environments? Polymers 13(16):2688

Goertzen WK, Kessler MR (2007) Dynamic mechanical analysis of carbon/epoxy composites for structural pipeline repair. Compos B 38(1):1–9. https://doi.org/10.3390/polym13162688

Harnnecker F, Rosa DS, Lenz DM (2012) Biodegradable polyester-based blend reinforced with curauá fiber: thermal, mechanical and biodegradation behaviour. J Polym Environ 20(1):237–244. https://doi.org/10.1007/s10924-011-0382-5

Hukins DWL, Mahomed A, Kukureka SN (2008) Accelerated aging for testing polymeric biomaterials and medical devices. Med Eng Phys 30(10):1270–1274. https://doi.org/10.1016/j.medengphy.2008.06.001

Hutchinson JM (1995) Physical aging of polymers. Prog Polym Sci 20(4):703–760. https://doi.org/10.1016/0079-6700(94)00001-I

Lee JS, Hwang GH, Kwon YS, Jeong YG (2020) Impacts of cellulose nanofibril and physical aging on the enthalpy relaxation behavior and dynamic mechanical thermal properties of poly(Lactic Acid) composite films. Polymer 202:122677. https://doi.org/10.1016/j.polymer.2020.122677

Luckachan GE, Pillai CKS (2011) Biodegradable polymers- a review on recent trends and emerging perspectives. J Polym Environ 19(3):637–676. https://doi.org/10.1007/s10924-011-0317-1

Matečić Mušanić S, Sućeska M (2009) Artificial ageing of double base rocket propellant: EEEffect on dynamic mechanical properties. J Therm Anal Calorim 96(2):523–529. https://doi.org/10.1007/s10973-008-9044-9

Mysiukiewicz O, Barczewski M, Skórczewska K, Matykiewicz D (2020) Correlation between processing parameters and degradation of different polylactide grades during twin-screw extrusion. Polymers 12(6):1333. https://doi.org/10.3390/polym12061333

Nampoothiri KM, Nair NR, John RP (2010) An overview of the recent developments in polylactide (PLA) research. Bioresour Technol 101(22):8493–8501. https://doi.org/10.1016/j.biortech.2010.05.092

Niaounakis M, Kontou E, Xanthis M (2011) Effects of aging on the thermomechanical properties of poly(Lactic Acid). J Appl Polym Sci 119(1):472–481. https://doi.org/10.1002/app.32644

Nofar M, Sacligil D, Carreau PJ, Kamal MR, Heuzey MC (2019) Poly (Lactic Acid) blends: processing, properties and applications. Int J Biol Macromol 125:307–360. https://doi.org/10.1016/j.ijbiomac.2018.12.002

Patti A, Cicala G, Acierno S (2021) Rotational rheology of wood flour composites based on recycled polyethylene. Polymers 13(14):2226. https://doi.org/10.3390/polym13142226

Patti A, Acierno S, Cicala G, Tuccitto N, Acierno D (2022a) Refining the 3D printer set-up to reduce the environmental impact of the fused deposition modelling (Fdm) technology. Chem Eng Trans 91:415–420. https://doi.org/10.3303/CET2291070

Patti A, Acierno S, Cicala G, Zarrelli M, Acierno D (2022b) Recovery of waste material from biobags: 3D printing process and thermomechanical characteristics in comparison to virgin and composite matrices. Polymers 14(10):1943. https://doi.org/10.3390/polym14101943

Patti A, Acierno S, Cicala G, Zarrelli M, Acierno D (2022c) The understanding the processing window of virgin and recycled bio-based filaments for 3D printing applications. Macromol Symp 405(1):2100291. https://doi.org/10.1002/masy.202100291

Patti A, Acierno S, Cicala G, Acierno D (2023) Predicting the printability of poly(Lactide) acid filaments in fused deposition modeling (FDM) technology: rheological measurements and experimental

evidence. ChemEngineering 7(1):1. https://doi.org/10.3390/chemengineering7010001

Paunonen S, Berthold F, Immonen K (2020) Poly(Lactic Acid)/pulp fiber composites: the effect of fiber surface modification and hydrothermal aging on viscoelastic and strength properties. J Appl Polym Sci 137(42):49617. https://doi.org/10.1002/app.49617

Peng Y, Wu P, Yang Y (2003) Two-dimensional infrared correlation spectroscopy as a probe of sequential events in the diffusion process of water in poly(ε-Caprolactone). J Chem Phys 119(15):8075–8079. https://doi.org/10.1063/1.1610441

Piemonte V, Sabatini S, Gironi F (2013) Chemical recycling of PLA: a great opportunity towards the sustainable development? J Polym Environ 21(3):640–647. https://doi.org/10.1007/s10924-013-0608-9

Pluta M, Murariu M, Alexandre M, Galeski DP (2008) Polylactide compositions. The influence of ageing on the structure, thermal and viscoelastic properties of PLA/calcium sulfate composites. Polym Degrad Stab 93(5):925–931. https://doi.org/10.1016/j.polymdegradstab.2008.02.001

Pokhrel G, Gardner DJ, Han Y (2021) Properties of wood-plastic composites manufactured from two different wood feedstocks: wood flour and wood pellets. Polymers 13(16):2769. https://doi.org/10.3390/polym13162769

Pop MA, Croitoru C, Bedő T, Geaman V, Radomir I, Coșnița M, Zaharia SM, Chicoș LA, Miloșan I (2019) Structural changes during 3D printing of bioderived and synthetic thermoplastic materials. J Appl Polym Sci 136(17):47382. https://doi.org/10.1002/app.47382

Regazzi A, Corn S, Ienny P, Bénézet JC, Bergeret A (2016) Reversible and irreversible changes in physical and mechanical properties of biocomposites during hydrothermal aging. Ind Crops Prod 84:358–365. https://doi.org/10.1016/j.indcrop.2016.01.052

Rocca-Smith JR, Chau N, Champion D, Brachais CH, Marcuzzo E, Sensidoni A, Piasente F, Karbowiak T, Debeaufort F (2017) Effect of the state of water and relative humidity on ageing of PLA films. Food Chem 236:109–119. https://doi.org/10.1016/j.foodchem.2017.02.113

Sachan R, Warkar SG, Purwar R (2022) An overview on synthesis, properties and applications of polycaprolactone copolymers, blends & composites. Polym Plast Technol Mater 62(3):327–358. https://doi.org/10.1080/25740881.2022.2113890

Schramm C (2020) High temperature ATR-FTIR characterization of the interaction of polycarboxylic acids and organotrialkoxysilanes with cellulosic. Mater Spectrochim Acta Part A 243:118815. https://doi.org/10.1016/j.saa.2020.118815

Sharma V, Sehgal R, Gupta R (2021) Polyhydroxyalkanoate (PHA): properties and modifications. Polymer 212:123161. https://doi.org/10.1016/j.polymer.2020.123161

Shojaeiarani J, Bajwa DS, Rehovsky C, Bajwa SG, Vahidi G (2019) Deterioration in the physico-mechanical and thermal properties of biopolymers due to reprocessing. Polymers. https://doi.org/10.3390/polym11010058

Signori F, Coltelli MB, Bronco S (2009) Thermal degradation of poly(Lactic Acid) (PLA) and poly(Butylene Adipate-Co-terephthalate) (PBAT) and their blends upon melt processing. Polym Degrad Stab 94(1):74–82. https://doi.org/10.1016/j.polymdegradstab.2008.10.004

Stark W (2013) Investigation of the curing behaviour of carbon fibre epoxy prepreg by dynamic mechanical analysis DMA. Polym Test 32(2):231–239. https://doi.org/10.1016/j.polymertesting.2012.11.004

Stoleru E, Hitruc EG, Vasile C, Oprică L (2017) Biodegradation of poly(Lactic acid)/chitosan stratified composites in presence of the phanerochaete chrysosporium fungus. Polym Degrad Stab 143:118–129. https://doi.org/10.1016/j.polymdegradstab.2017.06.023

Yarahmadi N, Jakubowicz I, Enebro J (2016) Polylactic acid and its blends with petroleum-based resins: effects of reprocessing and recycling on properties. J Appl Polym Sci 133(36):43916–43925. https://doi.org/10.1002/app.43916

Zhang C, Wang P, Ma CA, Wu G, Sumita M (2006) Temperature and time dependence of conductive network formation: dynamic percolation and percolation time. Polymer 47(1):466–473. https://doi.org/10.1016/j.polymer.2005.11.053

Publisher's Note Springer Nature remains neutral with regard to jurisdictional claims in published maps and institutional affiliations.